Numerical simulation of processes in gas discharge fast-flow CO_2 lasers

R.S. Galeev and R.K. Safiullin

Kazan State Architectural Construction Academy
Scientific Research Institute of Mathematics and Mechanics at Kazan State University

Received December 11, 2003

The paper discusses the results of numerical simulation of the processes in discharge chambers (DC) of the fast-flow CO_2 lasers. The conditions of axial glow discharge in conical- and parallelepiped-shaped DCs are under study. It is shown that the output power and efficiency of the CO_2 lasers can be increased by using conical tubes narrowed in the anode–cathode direction. For the parallelepiped-shaped DCs, two-dimensional flow in the narrow-channel approximation is considered. Two-dimensional distributions of vibrational and gas temperatures, as well as the degree of gas ionization inside DC, have been obtained.

Development of efficient numerical methods for studying basic processes proceeding in the gas discharge CO_2 lasers is motivated by a search for optimal modes of laser operation. Despite many-year efforts in this direction, the problem is actual until recently.

This paper is devoted to numerical simulation of processes in discharge chambers (DCs) of the fast-flow CO_2 lasers. The study is performed for conditions of axial glow discharge in DC with conical- (Fig. 1*a*) and parallelepiped-shaped (Fig. 1*b*) tubes. For DCs of the first type, we considered quasi-one-dimensional flow within four-temperature model of vibrational relaxation. This study pursues our earlier work,[1] where the superiority of conical-shaped discharge tubes was first forecasted. We have calculated distributions of gas dynamics parameters, concentrations of charged components of the gas discharge plasma, the along-DC intensity of the electric field, and the output power of the CO_2 laser. The influence of the laser channel shape on the output laser energy has been analyzed and the results are compared with the available experimental data.

For the rectangular-shaped DCs, we considered a two-dimensional flow in the narrow-channel approximation within a six-temperature model of the vibrational relaxation. It is shown that, in contrast to three- or four-temperature models, this model produces temperatures of symmetrical and deformation vibrational modes of CO_2 differing by more than 100 K. We calculated two-dimensional distributions of translational-rotational and vibrational temperatures, as well as degrees of gas ionization inside the DC.

1. Mathematical models

1.1. CO_2 lasers with conical-shaped tube

The mathematical model of the CO_2 laser with conical-shaped tube (Fig. 1*a*) involves the equations of glow discharge:

$$\frac{\mathrm{d}\, j_\mathrm{e}}{\mathrm{d}x} = k_i j_\mathrm{e} - k_\mathrm{a} j_\mathrm{e} - e\beta_\mathrm{e} n_\mathrm{e} n_+ + e k_\mathrm{d} N n_- - j_\mathrm{e} \frac{S'}{S}, \quad (1)$$

$$\frac{\mathrm{d}\, j_+}{\mathrm{d}x} = -k_i j_\mathrm{e} + e\beta_\mathrm{e} n_\mathrm{e} n_+ + e\beta_i n_+ n_- - j_+ \frac{S'}{S}, \quad (2)$$

$$\frac{\mathrm{d}\, j_-}{\mathrm{d}x} = k_\mathrm{a} j_\mathrm{e} - e\beta_i n_+ n_- - e k_\mathrm{d} N n_- - j_- \frac{S'}{S}, \quad (3)$$

$$\frac{\mathrm{d}E}{\mathrm{d}x} = \frac{e}{\varepsilon_0}(n_\mathrm{e} - n_+ + n_-) - E\frac{S'}{S}, \quad (4)$$

where x is the coordinate counted off cathode in the anode direction; j_e, j_+, j_- are the densities of electron current, as well as positive and negative ions, respectively; E is the intensity of electric field; $S = S(x)$ is the cross section of the discharge tube; e is the absolute value of the electron charge; and the other designations are conventional.

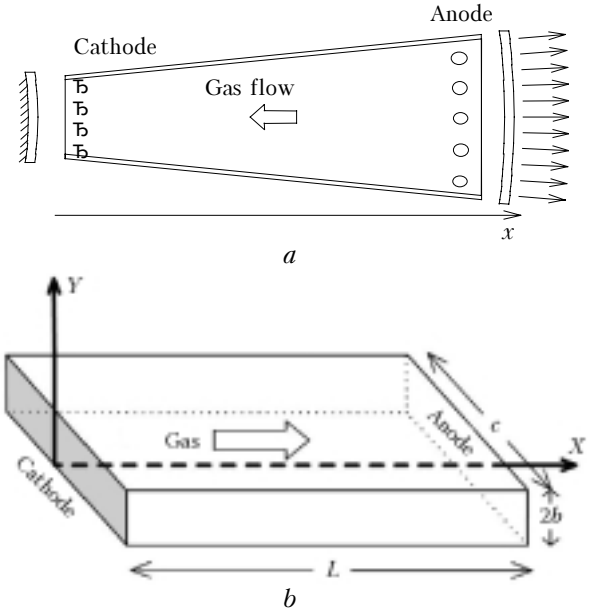

Fig. 1. CO_2 laser with (*a*) conical-shaped tube and (*b*) with the parallelepiped-shaped DC.

0235-6880/04/02–03 203-05 $02.00

Electron and positive ion current densities satisfy the following boundary conditions at electrodes:

$$j_e(0,t) = \gamma j_+(0,t), \quad j_-(0,t) = j_+(L,t) = 0, \qquad (5)$$

while the intensity of the electric field is related to the voltage drop across the discharge gap by the equality

$$\int_0^L E(x)\mathrm{d}x = U. \qquad (6)$$

The quasi-one-dimensional vibrationally non-equilibrium flow of the inviscid laser mixture CO_2–N_2–He in the tube is described by the equations

$$\rho u S = G = \text{const}, \qquad (7)$$

$$\rho u \frac{\mathrm{d}u}{\mathrm{d}x} = -\frac{\mathrm{d}p}{\mathrm{d}x}, \qquad (8)$$

$$\frac{\mathrm{d}u(E_g + p)}{\mathrm{d}x} = W_e - gI_{rad} - u(E_g + p)\frac{S'}{S}, \qquad (9)$$

$$p = \rho RT. \qquad (10)$$

where W_e is the power per unity volume; g is the laser amplification coefficient at $P(20)$ transition; I_{rad} is the laser radiation intensity.

The specific gas energy is defined as

$$E_g = \frac{p}{\kappa - 1} + \frac{\rho u^2}{2} + \rho e_{vib}. \qquad (11)$$

Here ρ is the gas mixture density; u is the gas mixture velocity; p is the gas pressure; R is the gas constant; G is the gas mass consumption through DC; $\kappa = c_p/c_v$; and e_{vib} is the specific vibrational energy of the gas mixture.

The equations of the vibrational relaxation are written in approximation of the four-temperature model as:

$$\frac{\mathrm{d}E_i}{\mathrm{d}x} = \frac{1}{u}w_i(p,T,E_2,E_3,E_4,\delta_i,E,j_e) = f_i, \quad i = 2,\ 3,\ 4, \qquad (12)$$

where E_i is the energy of the ith vibrational mode per unit volume. It was assumed that the symmetric ($i = 1$) and deformation ($i = 2$) vibrational modes of CO_2 are in equilibrium with each other. The values $i = 3$ and $i = 4$ correspond to antisymmetric vibrational mode of CO_2 and vibrational mode of N_2, respectively. Here δ_i is the part of the pumping energy incoming to the ith vibrational mode; the function w_i describes the right part of the kinetic equation for this mode.

The rate constants for excitation and ionization of molecules, as well as dissociation attachment and detachment of electrons are obtained from calculation of the electron energy distribution function (EEDF) for given values of the reduced intensity of the electric field E/N (N is the summarized concentration of atoms and molecules).

1.2. CO_2 lasers with the parallelepiped-shaped DC

We studied the processes in the positive column of the glow discharge in the narrow parallelepiped-shaped flow DCs (Fig. 1*b*). The gas flowed from cathode to anode. The DCs were defined by the planes $x = 0$, $x = L$, $y = 0$, $y = 2b$, $z = 0$, and $z = c$. The case under consideration, $b/c \ll 1$, assumed a homogeneity of the processes in the direction of Z-axis. We studied the processes in the mixtures CO_2–N_2–He–CO.

For the DCs, we solved the following set of equations:

$$\frac{\partial \rho u}{\partial x} + \frac{\partial \rho v}{\partial y} = 0; \qquad (13)$$

$$\rho u \frac{\partial u}{\partial x} + \rho v \frac{\partial u}{\partial y} = -\frac{\partial p}{\partial x} + \frac{\partial}{\partial y}\mu \frac{\partial u}{\partial y}; \qquad (14)$$

$$c_p \rho u \frac{\partial T}{\partial x} + c_p \rho v \frac{\partial T}{\partial y} = \frac{\partial}{\partial y}\lambda \frac{\partial T}{\partial y} + \mu\left(\frac{\partial u}{\partial y}\right)^2 + u\frac{\partial p}{\partial x} + \delta \mathbf{jE} + \varphi(E_1,E_2,E_3,E_4,E_5); \qquad (15)$$

$$p = NkT; \qquad (16)$$

$$G = 2c\int_0^b \rho u \mathrm{d}y; \qquad (17)$$

$$I = 2c\, eE\mu_e \int_0^b n_e \mathrm{d}y; \qquad (18)$$

$$\frac{\partial}{\partial y} D_a \frac{\partial n_e}{\partial y} - \frac{\partial n_e u}{\partial x} - \frac{\partial n_e v}{\partial y} + \nu_i n_e - \beta n_e^2 + q = 0, \qquad (19)$$

$$u\frac{\partial E_i}{\partial x} + v\frac{\partial E_i}{\partial y} = k_i \mathbf{jE} + f_i(T,E_1,E_2,E_3,E_4,E_5), \quad (i = 1-5), \qquad (20)$$

where v, μ, and λ are the vertical component of the flow velocity, the dynamical viscosity and thermal conductivity of the gas mixture; δ is the part of pump power contributing into translational-rotational degrees of freedom of molecules; I is the total current; μ_e is the mobility of electrons; D_a is the coefficient of ambipolar diffusion of electrons; ν_i is the frequency of ionization; β is the coefficient of the electron–ion recombination; E_i is the energy of ith vibrational mode per unit volume; δ_i is the part of pump energy contributing into the ith vibrational mode ($i = 5$ corresponds to the vibrational mode of the CO constituent).

Equations of vibrational kinetics (20) are written in the six-temperature approximation. They include the convective and diffusion transport of vibrational energy, as well as electron-induced excitation of molecule vibrations and $(V-V)$, $(V-V')$, $(V-T)$ processes. The functions φ and f_i also depend on the rates of $(V-V)$, $(V-V')$, and $(V-T)$ processes. They can be obtained as described in Ref. 2.

The boundary conditions were formulated as follows. At the DC input, we set:

$$T|_{x=0} = T(0,y),\ u|_{x=0} = u(0,y),$$

$$v|_{x=0} = 0,\ n_e|_{x=0} = n_e(0,y),\ E|_{x=0} = E_0. \quad (21)$$

It was assumed that the excitation of molecular vibrations is equilibrium.

It was assumed that at the DC walls

$$u|_{y=0} = u|_{y=2b} = 0,\ v|_{y=0} = v|_{y=2b} = 0\ ,$$

$$n_e/N|_{y=0} = n_e/N|_{y=2b} = 10^{-10};$$

$$T_1(x,0) = T_1(x,2b) = T_2(x,0) = T_2(x,2b) = T(x,0);$$

$$\frac{\partial T_3}{\partial y}(x,0) = \frac{\partial T_3}{\partial y}(x,2b) = \frac{\partial T_4}{\partial y}(x,0) = \frac{\partial T_4}{\partial y}(x,2b) =$$

$$= \frac{\partial T_5}{\partial y}(x,0) = \frac{\partial T_5}{\partial y}(x,2b) = 0. \quad (22)$$

The following conditions were put on the symmetry plane ($y = b$):

$$\frac{\partial u}{\partial y} = \frac{\partial v}{\partial y} = \frac{\partial n_e}{\partial y} = \frac{\partial T}{\partial y} = \frac{\partial E_1}{\partial y} = \frac{\partial E_2}{\partial y} =$$

$$= \frac{\partial E_3}{\partial y} = \frac{\partial E_4}{\partial y} = \frac{\partial E_5}{\partial y} = 0,\ \ v = 0. \quad (23)$$

The viscosity and the coefficient of thermal conductivity of the gas mixture were calculated from the formulae as given in Ref. 3. Their temperature dependences were represented in the form

$$\frac{\mu}{\mu_0} = \frac{\lambda}{\lambda_0} = (T/T_0)^{0.7},\ \lambda_0 = \lambda(T_0),\ \ \mu_0 = \mu(T_0). \quad (24)$$

2. Numerical method

2.1. CO_2 lasers with conical-shaped tubes

At the DC input, we specified the pressure, velocity, and temperature and assumed some equilibrium between translational-rotational and vibrational degrees of freedom of molecules. In a particular case of the cylindrical-shaped tube, we used the model of the Fabry–Perot resonator in the constant intensity approximation. For the conical tube, we used the model of the spherical-concentric resonator in the approximation $I(x) = I(0)S(0)/S(x)$. The average gain was calculated by the formula

$$\bar{g} \equiv \frac{1}{L}\int_0^L g\,dx = \frac{1}{2L}\ln\frac{1}{r_1 r_2}, \quad (25)$$

where $r_1 = 1 - a_1$ and $r_2 = 1 - a_2 - \theta$ are the reflection coefficients of the mirrors; a_1 and a_2 are the absorption coefficients of the mirrors; θ is the transmissivity of the exit mirror; L is the distance between the mirrors (assumed to be equal to the cathode/anode distance). The laser output power was calculated by the formula

$$P_{rad} = \frac{\theta \bar{g} I(L) S(L) L}{(1 + \sqrt{r_1/r_2})(1 - \sqrt{r_1 r_2})}. \quad (26)$$

The intricate system of differential equations was solved by the method of split into three subsystems describing different physical processes. First of all, the gas-dynamical parameters u, T, and p in the layer $x + \Delta x$ were calculated as described in Refs. 1 and 4. Then in the layer $x + \Delta x$ we calculated parameters E_k using an implicit scheme which was reduced to the iterative Newton method. This procedure was performed step by step in direction from cathode to anode. Then the system of equations (1)–(4) was solved along the entire DC using the matrix run method. To obtain a self-consistent solution, up to 10 global iterations were performed among the three subsystems.

2.2. Parallelepiped-shaped CO_2 lasers

Equations (13)–(15), (19)–(20) can be represented in the form

$$a_i \frac{\partial f_i}{\partial x} + b_i \frac{\partial f_i}{\partial y} = \frac{\partial}{\partial y}\left(c_i \frac{\partial f_i}{\partial y}\right) + d_i + e_i f_i,\ i = 1, 2, \ldots, 9; \quad (27)$$

$$\frac{\partial \rho u}{\partial x} + \frac{\partial \rho v}{\partial y} = 0. \quad (28)$$

Here the coefficients a_i, b_i, c_i, d_i, and e_i may depend on the functions f_j and on the derivatives of the functions f_k ($k \neq i$).

Equation (27) was approximated with the finite-difference equation

$$a_{i,m}^{n+1/2} \frac{f_{i,m}^{n+1} - f_{i,m}^{n}}{\Delta x} +$$

$$+ b_{i,m}^{n+1/2} \frac{s_i(f_{i,m+1}^{n+1} - f_{i,m-1}^{n+1}) + (1 - s_i)(f_{i,m+1}^{n} - f_{i,m-1}^{n})}{2\Delta y} =$$

$$= \frac{1}{\Delta y^2}\left\{\left[(1 - s_i)(f_{i,m+1}^{n} - f_{i,m}^{n}) + s_i(f_{i,m+1}^{n+1} - f_{i,m}^{n+1})\right] c_{i,m+1/2}^{n+1/2} -\right.$$

$$\left. -\left[(1 - s_i)(f_{i,m}^{n} - f_{i,m-1}^{n}) + s_i(f_{i,m}^{n+1} - f_{i,m-1}^{n+1})\right] c_{i,m-1/2}^{n+1/2}\right\} +$$

$$+ d_{i,m}^{n+1/2} + e_{i,m}^{n+1/2}[(1 - s_i) f_{i,m}^{n} + s_i f_{i,m}^{n+1}]. \quad (29)$$

Provided that $1/2 \le s_i \le 1$ and the coefficients a_i, b_i, c_i, d_i, and e_i are "frozen", this finite-difference scheme is absolutely stable.[5] If $f_{i,k}^{n}$, $a_{i,k}^{n+1/2}$, $b_{i,k}^{n+1/2}$, $c_{i,k}^{n+1/2}$, $d_{i,k}^{n+1/2}$, $e_{i,k}^{n+1/2}$ are known, then $f_{i,k}^{n+1}$ values can be obtained from equation (29) by the scalar run method taking into account the boundary conditions.

The transverse velocity component is obtained from the finite-difference equation

$$\frac{1}{2\Delta x}\left[(\rho u)_m^{n+1} - (\rho u)_m^n\right] + \frac{1}{2\Delta x}\left[(\rho u)_{m+1}^{n+1} - (\rho u)_{m+1}^n\right] +$$

$$+ \frac{1}{\Delta y}\left[(\rho v)_{m+1}^{n+1/2} - (\rho v)_m^{n+1/2}\right] = 0. \qquad (30)$$

If $f_{i,k}^{n+1}$ and ρ_k^{n+1} values have been already calculated, and the $v_0^{n+1/2}$ value is available from the boundary condition, then the $v_m^{n+1/2}$ values follow from equation (30) for $m = 1, \ldots, M$.

To calculate a_i, b_i, c_i, d_i, and e_i, which depend on the sought characteristics, the iterations should be invoked. For the first iteration, it is possible to set $f_{i,k}^{n+1} = f_{i,k}^n$. In our calculations, we used from 3 to 6 iterations.

3. Results and discussion

Numerical results for lasers with conical-shaped tubes are presented in Fig. 2. The cross section $S(L)$ of the tube near anode was 141 cm^2; at cathode $S(0)$ varied from $0.5S(L)$ to $2S(L)$. It was also assumed that

$$S(x) = \left(\frac{\sqrt{S(L)} - \sqrt{S(0)}}{L}\, x + \sqrt{S(0)}\right)^2. \qquad (31)$$

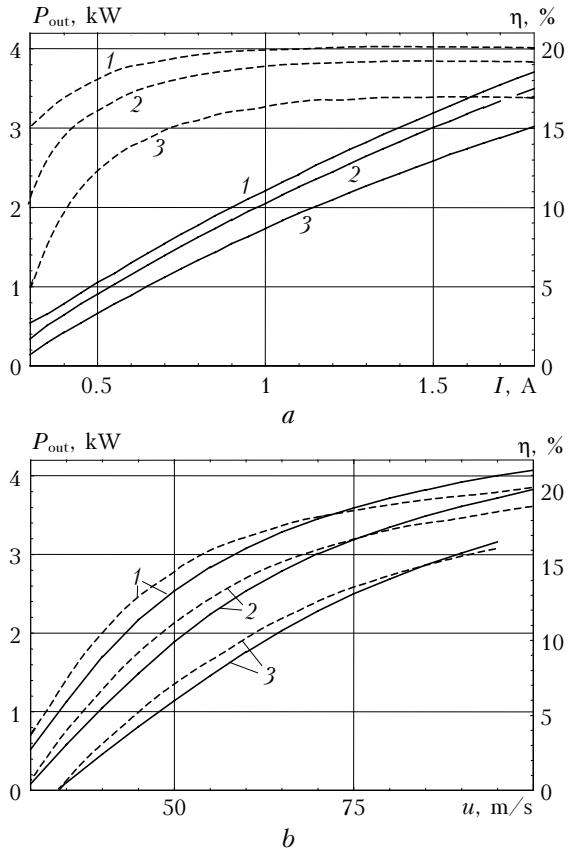

Fig. 2. Output power P_{out} (solid lines) and efficiency η of the laser (dashed lines) as functions of discharge current I (*a*) and as functions of flow rate u (*b*): $S(L)/S(0) = 2$ (curve *1*); $S(L)/S(0) = 1$ (curve *2*); and $S(L)/S(0) = 0.5$ (curve *3*).

The gas was directed from anode to cathode. We considered the gas mixture CO_2:N_2:He = 4.5:13.5:82. The DC parameters were close to those described in Ref. 6: $L = 60$ cm, the discharge current $I = 1.8$ A, the gas pressure at input $p = 30$ Torr, $|u| = 97$ m/s, and $T = 300$ K.

Fractions of power applied to the translational-rotational and vibrational degrees of freedom of molecules, as well as the rate constants of electron ionization and attachment to molecules, were obtained in the EEDF calculation.

The obtained results are presented in the Table.

Parameters	$\frac{S(L)}{S(0)} = 2$	$\frac{S(L)}{S(0)} = 1$	$\frac{S(L)}{S(0)} = 0.5$
Voltage drop, U, kV	10.22	10.15	9.94
Output energy, P_{out}, kW	3.72	3.50	3.04
Efficiency, η, %	20.24	19.14	17.01
Transmission coefficient of exit mirror θ, %	15.79	15.09	13.26

It is seen from the data presented in the Table, as well as from plots in Fig. 2, that the use of conical-shaped tubes, narrowed in the anode–cathode direction and the gas flowing from anode to cathode lead to a marked increase of the laser output power and efficiency.

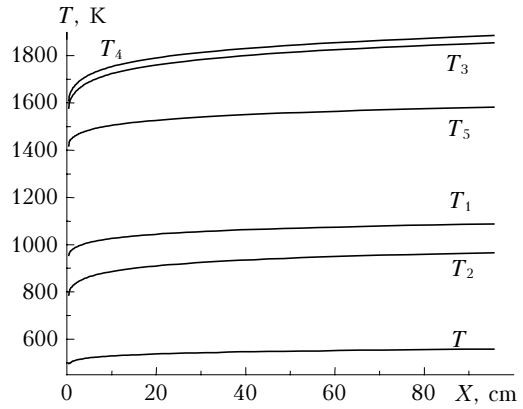

Fig. 3. Distributions of translational-rotational and vibrational temperatures along the DC ($y = b$).

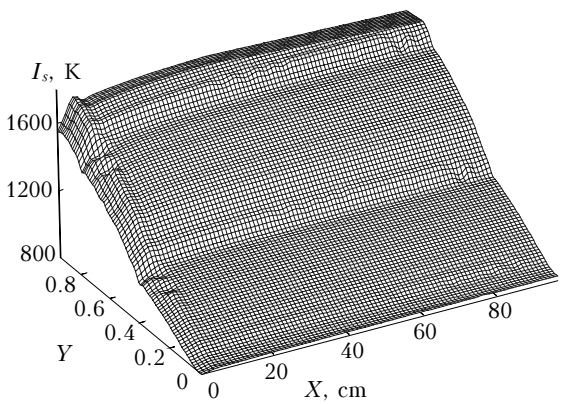

Fig. 4. Distribution of vibrational temperature T_3 of $(00V)$ mode of CO_2 inside DC.

For CO_2 lasers with the parallelepiped-shaped DCs, some calculation results for the mixture $CO_2 : N_2 : He : CO = 16 : 32 : 48 : 4$ are presented in Figs. 3 and 4. At the DC input we set: $T(0, y) = 300$ K, $p = 20$ Torr, $u = 100$ m/s. The boundary conditions at DC walls were used in the form:

$$T(x, 0) = 300 \text{ K}, \; E_1 = E_1(T(x, 0)), \; E_2 = E_2(T(x, 0)),$$

$$\partial E_3 / \partial y = \partial E_4 / \partial y = \partial E_5 / \partial y = 0; \; u = v = 0;$$

and the degree of the gas ionization in the form

$$\alpha \equiv n/N = 10^{-10}.$$

As is seen from Fig. 3, the six-temperature model gives a marked difference between temperatures of symmetrical and deformation modes of CO_2. As was noted in Ref. 3, in the framework of this model, the problem of "stiffness" of vibrational kinetics equations takes place. Therefore, most two-dimensional calculations were made in the approximation of the three- or four-temperature model, where manifestations of the "stiffness" are not so strong. In our calculations, this showed itself in the fact that in the $0 \le x \le 0.3$ cm region (not shown in the figures presented above), the basic parameters experienced considerable decaying oscillations. As is seen from Figs. 3 and 4, almost everywhere in DC in the symmetry plane ($y = b$) $T_3 > 1500$ K and a considerable population inversion takes place. As the result of calculations, two-dimensional distributions of gas-dynamics, kinetic, and electric characteristics of the CO_2 laser medium were also obtained.

References

1. R.S. Galeev, Proc. SPIE **2713**, 30–37 (1996).
2. K. Smith and R. Thomson, *Computer Modeling of Gas Lasers*, (Plenum Press, New York, 1978).
3. S. Sazhin, P. Wild, C. Leys, D. Toebaert, and E. Sazhina, J. Phys. D. **26**, 1872–1883 (1993).
4. Sh.F. Araslanov and R.K. Safiullinn, Quant. Electron. **31**, No. 8, 697–703 (2001).
5. V.M. Paskonov, V.I. Polezhaev, and L.A. Chudov, *Numerical Simulation of the Processes of Heat and Mass Exchange* (Nauka, Moscow, 1984), 286 pp.
6. R.A. Harry and D.R. Evans, IEEE J. Quant. Electron. **24**, No. 3, 503–506 (1988).